Effect of Wind on the Chemical Uptake Kinetics of a Passive Air Sampler

Xianming Zhang,[†] Trevor N. Brown,[†] Amer Ansari,[†] Beom Yeun,[†] Ken Kitaoka,[‡] Akira Kondo,[‡] Ying D. Lei,[†] and Frank Wania[†,*]

[†]Department of Chemistry and Department of Physical and Environmental Sciences, University of Toronto Scarborough, Toronto, Ontario M1C 1A4, Canada

[‡]Graduate School of Engineering, Osaka University, Suita, Osaka 565-0871, Japan

S Supporting Information

ABSTRACT: Passive air samplers (PASs) operate in different types of environment under various wind conditions, which may affect sampling rates and thus introduce uncertainty to PAS-derived air concentrations. To quantify the effect of wind speed and angle on the uptake in cylindrical PASs using XAD-resin as the sampling medium, we measured the uptake kinetics of polychlorinated biphenyls (PCBs) in XAD and of water in silica-gel, both under quasi wind-still condition and with lab-generated wind blowing toward the PASs at various speeds and angles. Passive sampling rates (PSRs) of PCBs under laboratory generated windy conditions were approximately 3−4 times higher than under wind-still indoor conditions. The rate of water uptake by silica-gel increased with wind speed, following a logarithmic function so that PSRs are more strongly influenced at lower wind speed. PSRs of both PCBs and water varied little with wind angle, which is consistent with computational fluid dynamic simulations showing that different angles of wind incidence cause only minor variations of air velocities within the cylindrical sampler housing. Because modifications of the design of the cylindrical PAS were not successful in eliminating the wind speed dependence of PSRs at low wind levels, indoor and outdoor deployments require different sets of PSRs. The effect of wind speed and angle on the PSRs of the cylindrical PAS are much smaller than what has been reported for the double-bowl polyurethane foam PAS. PSRs of the cylindrical XAD-PAS therefore tend to vary much less between sampling sites exposed to different wind conditions.
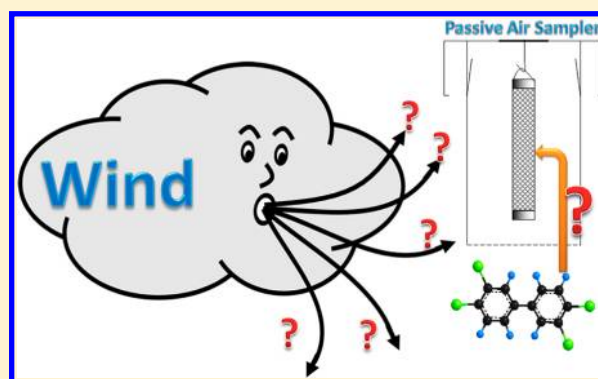
INTRODUCTION

Allowing for time-integrated monitoring of the air concentrations of semivolatile organic compounds (SVOCs) at low cost and without power requirement, passive air samplers (PASs) have seen increasing use over the past decades.[1,2] PASs have gained more popularity, especially since 2004 when the Stockholm Convention[3] came into force and various stakeholders became interested in evaluating its effectiveness in reducing levels of persistent organic pollutants in the global atmosphere. Having been used in several long-term monitoring campaigns, e.g. 4, PASs have proven effective in studying the interannual time trends of SVOCs in air. PASs have also found use in assessing spatial distributions of SVOCs at different scales[4−7] and identifying potential sources of, and human exposure to, SVOCs in various types of environments.[8−11]

Environmental conditions under which PASs are deployed can vary tremendously. For example, wind at sampling sites outdoors is generally much stronger and more variable than during indoor deployments[12] and due to differences in surface roughness, sites in urban or forested areas tend to be less windy than those in unobstructed locations.[13] Different wind conditions may impact passive sampling rates (PSRs). While

studies[14−16] on the double-bowl polyurethane foam (PUF)-disk PAS (PUF-PAS) by Harner et al.[17] suggested that the PAS housing can somewhat dampen the effect of wind, PSRs increased exponentially with wind speed,[14,15] especially when ambient wind speed exceeds 4 m/s (15 km/h), which is commonly observed in outdoor settings.[14,18,19] Such effects could possibly cause variations in the calibrated PSRs of the PUF-PAS by as much as an order of magnitude.[19]

In order to account for wind effects on PSRs, depuration compounds (DCs) have commonly been added to sampling media prior to deploying a PAS; site-specific PSRs are then derived from the loss kinetics of the DCs.[15] The loss rates of DCs and thus the DC-derived PSRs were found to correlate with wind speed.[14,15] The use of DCs rests on the assumption that "uptake is air-side controled" and "uptake and loss mass transfer directions are opposite to each other".[15] Recent studies have shown this requirement is unlikely to be satisfied because
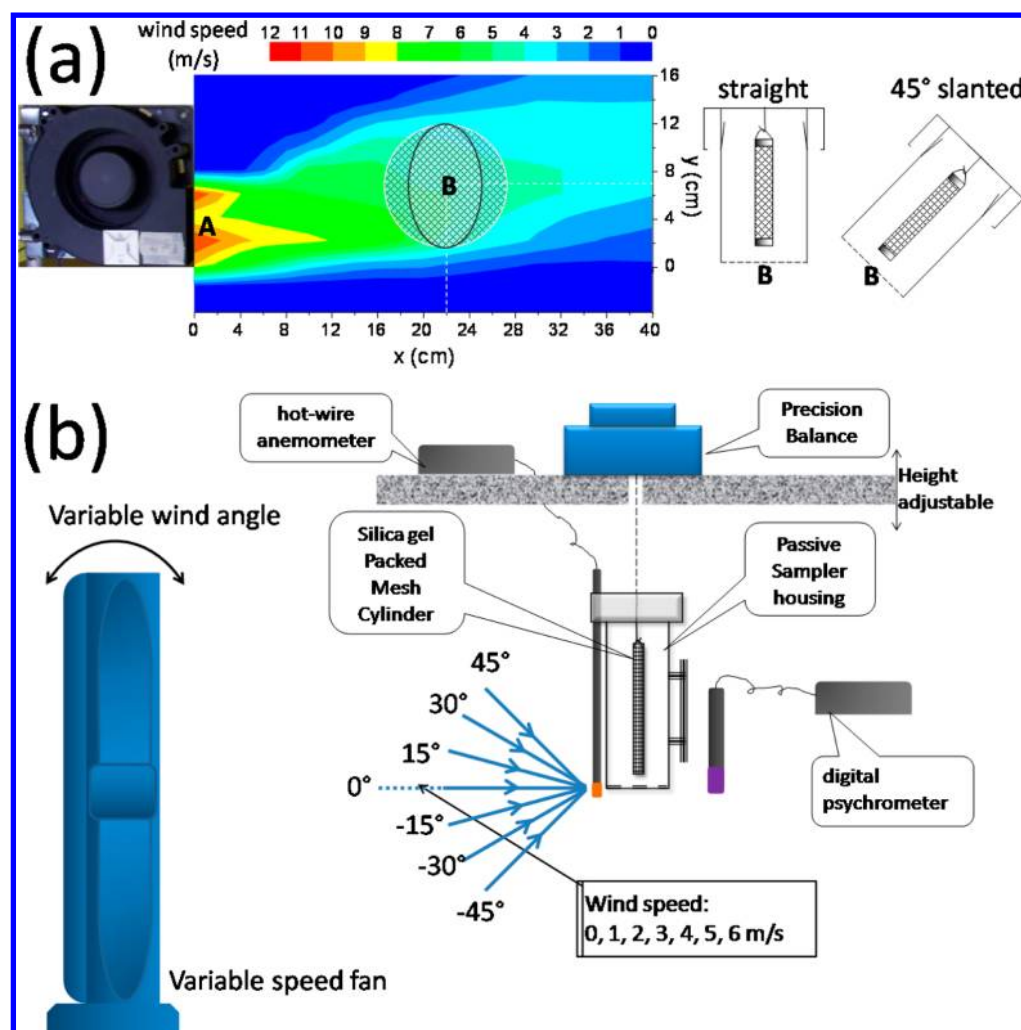
Figure 1. Spatial distribution of speed (m/s) of the lab-generated wind in the experiments measuring uptake of (a) PCBs in XAD-filled passive samplers and (b) water vapor uptake in silica gel-filled passive samplers. Wind speeds were measured with a hot-wire anemometer at a resolution of 2 cm. The round and elliptical rings in (a) represent the position (projective planes of the opening) of the straight and 45° slanted passive air samplers, respectively.

of the existence of a mass transfer resistance within porous passive sampling media that can affect the overall PSR.[20,21] An alternative approach to address the wind effect is to have the sampling medium better sheltered from the wind. For example, in order to reduce the effect of wind on PSRs, a thick porous membrane envelopes the sampling medium (sorbent) in the commercial Radiello-type PAS.[22,23] Mounting PUF-disks at the top of semienclosed cylindrical housings resulted in lower PSRs than in the double-bowl housing,[24] suggesting that a more deeply sheltered PUF-disk is less affected by ambient wind. While a few studies have focused on the wind effect on the PUF-PAS[14,15,18,25] or semipermeable membrane devices PAS,[26,27] studies quantitatively investigating the effect of wind on PSRs of the XAD-PAS are still very limited. A wind-tunnel study suggested little wind effect on the water uptake by silica-gel filled mesh cylinders at wind speed of 5−15 m/s,[28] but field deployments of XAD-PAS noted higher PSRs at sites exposed to very strong winds.[29,30]

Besides wind speed, the angle at which the wind is blowing at a PAS may also affect the PSR. This angle may be affected by the local terrain of the deployment site. For example, PASs deployed along a slope may have valley to mountain winds preferentially blowing at an angle toward it.[31] A recent study

showed that wind blowing at the double-bowl PUF-PASs at different angles caused variations in the uptake kinetics by as much as 80%.[25] No studies have tested the effect of wind angle on SVOC uptake by the cylindrical XAD-PAS. Whereas the gap between the two domes of the PUF-PAS allows for the entry of wind into the sampler housing and therefore the impingement of wind on the sorbent material, the semienclosed configuration of the XAD-PAS presumably prevents wind from passing through the sampler housing and interacting directly with the sorbent. Therefore, the influence of wind speed and angle on the sampling rates for the XAD-PAS could be different from that for the PUF-PAS and is thus worthy of further investigation.

In this study, we conducted experiments under controlled variable wind conditions indoors. PSRs for the uptake of polychlorinated biphenyls (PCBs) in XAD-filled mesh cylinders and the uptake of water vapor in silica-gel filled mesh cylinders were measured at different wind speeds and angles. We also modified the design of the XAD-PAS to explore whether the effect of wind on chemical uptake can be reduced. The experiments were complemented by computational fluid dynamics (CFD) simulations of the wind field within the

housing of the XAD-PAS to explore how it is affected by wind speed and angle.

MATERIALS AND METHODS

PCB Uptake by XAD-PASs under Different Wind Conditions. PCBs were selected as the target chemicals because their partition properties overlap with many SVOCs of environmental interest. Three sets of 12 XAD-based PAS[31] (short 10 cm version) each were simultaneously deployed in the same university office and retrieved in duplicates after 35, 67, 92, 112, 127, and 144 days. One set was deployed under quasi wind-still conditions (referred as wind-still condition hereafter although minor air flow around these PASs can be expected to have occurred due to building ventilation, human movement, door opening and closing, and the influence of the wind generated for the other sets of PASs deployed within the same room), and the other two had wind blowing at an angle of 0° and 45° toward the opening of the housing, respectively (Supporting Information (SI) Figure S1). The wind was generated using one electronic cooling fan (Delta Electronics Inc. BFC1212B, 12 V, 1.1A, 2800 rpm) for each sampler. The generated wind field measured on a horizontal plain parallel to the fans with a hot-wire anemometer (Kimo VT-200) is shown in Figure 1a. Based on the spatial distribution of wind generated by the fans and to mimic the average outdoor wind speed of ~4 m/s,[14] the center at the opening of the PAS housing was set up at point B (Figure 1a). Although wind speeds measured at point A had no significant difference ($p = 0.29$, Wilcoxon rank-sum test) between the straight PASs and the slanted PASs, the average wind speed measured at point B for the straight PASs was 4.3 ± 0.2 m/s, which was higher ($p < 0.001$) than the 3.6 ± 0.3 m/s for the slanted PASs (SI Figure S2). Air concentrations in indoor air during PAS calibration were measured with an active high-volume sampler (HVS) using glass fiber filter and PUF/XAD/PUF cartridge to sample particle-bound and gas-phase PCBs. Details on sampling, sample extraction, measured concentrations, and a discussion of the uncertainties are presented in the SI.

XAD Preparation and Extraction. Previously used XAD-2 resin was Soxhlet extracted with dichloromethane two times (~24 h each) before being used as the sampling medium. Upon retrieval, the XAD-filled mesh cylinders were stored in airtight metal tubes at −20 °C until extraction. After spiking with 100 μL of a solution containing 0.25 ng/μL of $^{13}C_{12}$-labeled PCB congeners 77, 101, 141, and 178 (Cambridge Isotope Laboratories) as surrogate standards, each sample was Soxhlet extracted for 24 h with ~500 mL dichloromethane. Extracts were rotoevaporated to ~2 mL and eluted through dehydrated sodium sulfate packed in a disposable pasteur pipet to remove moisture. The eluent was blown down with high purity (5.0) nitrogen, solvent exchanged to iso-octane and reduced to ~0.5 mL in a vial, to which 100 ng mirex was added as internal standard for quantification.

Instrumental Analysis. PCBs were analyzed with an Agilent 6890 gas chromatograph coupled with a 7683 autosampler and a 5973 mass spectrometric detector. 1.0 μL of extract was injected in splitless mode (injector temperature 250 °C) and separated using a DB5-MS capillary column (60 m length × 0.25 mm i.d., 0.25 μm film thickness, J&W Scientific) with helium (1.4 mL/min) as carrier gas. The chromatograph's oven temperature was 80 °C for 1 min, increased to 160 °C at 10 °C·min^{-1}, then to 280 °C at 3 °C·min^{-1}, which was held for another 6 min. Temperatures for the ion source and

quadrupole of the mass spectrometer were 230 and 150 °C. The mass spectrometer was operated with electron impact ionization (70 eV) and selective ion monitoring. The quantitative and qualitative ions monitored are listed in SI Table S1.

QA/QC. Recoveries of the PCBs as indicated by the four surrogate standards ranged 67−156% (interquartile range <20%). No PCBs were detected in the solvent blanks, which were included in every batch (5 samples) of Soxhlet extractions. One field blank had levels of PCB-52, -49, -74, -99, -101, -110, -153 at 5−15% of the samples. The other three field blanks contained less than 5% of the PCB amounts in the samples. Because the recoveries and blank levels were smaller than the variability of trace organic contaminant analysis, the reported values were neither recovery nor blank corrected. Relative differences in PCB levels between duplicates were $42\% \pm 2\%$, $17\% \pm 11\%$, and $22\% \pm 17\%$ for the wind-still, straight, and slanted conditions, respectively. The large relative difference for the duplicates under wind-still conditions are sample and compound independent. As all samples were handled by the same personnel, the possibility of larger variations originating from differences in sample preparation and analysis are low. With information gained from this study, we attribute the larger relative difference between duplicates to the higher sensitivity of PSRs to wind at low wind speed (discussed in detail below).

Coefficient of variance of the wind speeds in the experimental setup was 4% at point A of Figure 1a for all PASs, 4% and 8% at point B for the straight and slanted PASs, respectively. The wind speeds (measured at position A, Figure 1a) for the 24 fans after running for 100 days were 87−103% of that measured at the beginning of the experiment.

Water Uptake by Silica-Gel under Different Wind Conditions. Passive sampling of water vapor from air using silica-gel filled mesh cylinders as the sampling medium is an effective approach to investigate effects on PSRs by factors that are independent of sampled chemicals and sampling medium.[32] The same gravimetric approach as in a previous study[32] was used to measure the kinetics of water uptake under different wind conditions: the mass gain of a silica-gel filled mesh cylinder suspended from an analytical balance is recorded repeatedly and can be converted into a sampling rate if the water vapor concentration is known from measurements of relative humidity and temperature. Wind was generated using a large fan (Mastercraft FE6-T2, 66 cm in diameter) placed in an open corridor that served as a wind tunnel. This approach is similar to that by Tuduri et al.[14] Air velocities between 1 and 6 m/s at the PAS were achieved by varying fan speed and the distance between fan and PAS. To ensure constant wind conditions during the experiment, wind speed was regularly recorded with a hot-wire anemometer (Kimo VT-200) positioned at the opening of the PAS. Because wind flow caused the balance reading to become unstable, prior to recording mass each minute, the fan was automatically switched off for 30 s with a programmable Arduino controlling board (Arduino UNO) to stabilize the balance (referred as half-wind condition hereafter). Each experiment with half-wind conditions was followed by an experiment with wind-still conditions so that the PSRs under continuous wind could be derived from the difference in the PSRs recorded during half-wind and wind-still conditions (SI Figure S3). All the PSRs reported here have been adjusted for continuous wind. The wind conditions studied included wind with different speeds (1, 2, 3, 4, 5, 6 m/s) blowing at 0° toward the opening of the PAS

(Figure 1b) and wind of 3 m/s blowing at angles of $\pm 15°$, $\pm 30°$, and $\pm 45°$ at the PAS. Measurements were replicated five times for each wind condition and the coefficients of variance were <15%.

Sampler Design Modifications and Wind Influence Test. Several modifications were made to the design of the XAD-PAS developed by Wania et al.[28] (design A in SI Figure S4) with the intention to reduce the influence of wind on PSRs. The coarse mesh at the sampler housing opening was replaced in designs B, C, and D with honeycomb metal sheets with smaller openings (details in SI Table S2). Two designs are further modified from design D by covering half of the bottom opening with a metal sheet: Design E had the outer ring of the opening covered such that only the center of the bottom is perforated, whereas design F had the center of the bottom covered and the outer ring perforated. Both designs E and F had the same open area. Design G was inspired by the commercial Radiello PAS: It was comprised of a silica gel filled mesh cylinder (2 cm diameter, 10 cm in height) placed in a bigger empty mesh cylinder (3 cm in diameter). Design H had the outer mesh cylinder from design G wrapped in tissue paper (Kimwipe) to further reduce wind turbulence in the layer of air right adjacent to the gel-filled sampling cylinder. Designs G and H used the original housing. Design I had three layers of inner flaps whereby the first and third layers covered half the cross-sectional area of the opening from the edge, and the second layer covered the same area, but at the center of the shelter. Silica-gel packed mesh cylinders were put in the modified PASs and water uptake was measured under windy (4 m/s at 0° angle) and wind-still conditions using the same gravimetric approach described above.

Computational Fluid Dynamics Simulation. Wind fields within the sampler housing under the two ambient wind conditions corresponding to the PCB uptake experiment were assessed via computational fluid dynamics (CFD) simulations. Additionally, CFD simulations were performed to investigate how ambient wind speed and angle affect the wind field inside the PAS, particularly the wind speed surrounding the passive sampling medium. The CFD simulations were based on the continuity equation and conservation equations for mass and momentum. The standard k-ε turbulent model for high Reynolds number was adopted. The wall function was adopted on the surface of the PAS housing. All equations were solved by the semi-implicit method for pressure linked equations (SIMPLE Algorithm). The domain selected for the calculations was large enough so that the ambient wind is not influenced by the PAS.

■ RESULTS AND DISCUSSION

Effect of Wind Speed on Uptake in Cylindrical Passive Sampler. *Wind Effect on PCB Uptake by XAD.* Air concentrations of PCBs from the HVS measurements (SI Table S3) and the amounts accumulated in XAD-PASs at different deployment times (SI Table S4) were used to derive PSRs for PCBs of 0.13−0.33 and 0.44−1.16 m³/d at wind-still and 0° windy conditions (wind speed 4.3 ± 0.2 m/s at the center of the PAS opening) respectively (SI Table S5). Uptake of PCBs was faster under windy conditions (Figure 2, SI Figure S5). The ratio between the PSRs under windy (4 m/s) and wind-still (~0 m/s) conditions can serve as a quantitative measure of the wind effect and is independent of any potential error in the measured indoor air concentrations. This wind enhancement factor WEF$_{4:0}$ for the uptake of PCBs in XAD-
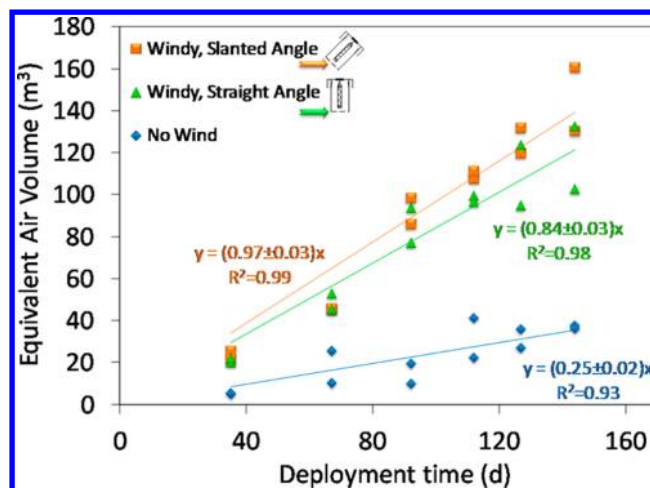
**Figure 2.** Passive air sampling kinetics (Penta-CB110 as an example) for samplers under windy (lab generated wind blowing at 45° angle and at 0° angle toward the cylindrical passive air samplers) and wind-still conditions.

filled cylindrical PAS was 3.3 ± 0.2 with the wind blowing at a straight angle at the PAS.

Wind Effect on Water Uptake by Silica-Gel. As was the case for PCB uptake, the PSRs for water vapor under all windy conditions (Figure 3) were significantly higher than under wind-still condition (Wilcoxon rank-sum test, $p < 10^{-6}$). At a wind angle of 0° and various wind speeds from 0 to 6 m/s, PSRs increased with ambient wind speed (Figure 4). The increase was much larger at lower wind speeds: the PSRs at 1 m/s were about double of the PSRs at wind-still condition (0 m/s), whereas PSRs only increased by 30% within the wind speed range from 1 to 6 m/s. Within such a range of wind speed, the relationship between PSR and wind speed ($v_{ambient}$) is well described by a logarithmic function:

$$PSR/(m^3/d) = \ln[10.25(\pm 0.47)v_{ambient}/(m/s) + 4.27(\pm 0.17)], \ R_{adj}^2 = 0.964 \quad (1)$$

Similar relationships between PSR and wind speed have also been found for the Radiello PAS.[22,23] Note that this empirical equation should not be extrapolated beyond the experimental range to very high wind speeds. Even if the air-side mass transfer resistance reaches an infinitesimally small value as wind speed increases, the PSR will not approach infinity due to the mass transfer resistance in the sampling media. The higher sensitivity of PSR to wind for the XAD-PAS at lower wind speed is consistent with the mechanistic understanding of uptake kinetics. In a sensitivity analysis on a PAS model we developed recently (Figure S7 of ref 21), the PSR was found to be more sensitive to boundary layer thickness (and thus wind speed) if the boundary layer thickness is high (corresponding to lower wind speed). The experimental results show lower sensitivity of PSR to wind as the wind speed gets higher, which can explain why a previous study relying on a similar experimental approach but at a lower temperature (12−15 °C) found the PSR (~3.5 m³/d) insensitive to wind speed within the range from 5 to 15 m/s,[28] while PSRs of XAD-PAS deployed indoors and outdoors deviate notably.[28,32,33] Furthermore, when deployed indoors where the wind speed is low, even small wind variations could lead to a notable change in PSRs. The high sensitivity of the PSR to wind at
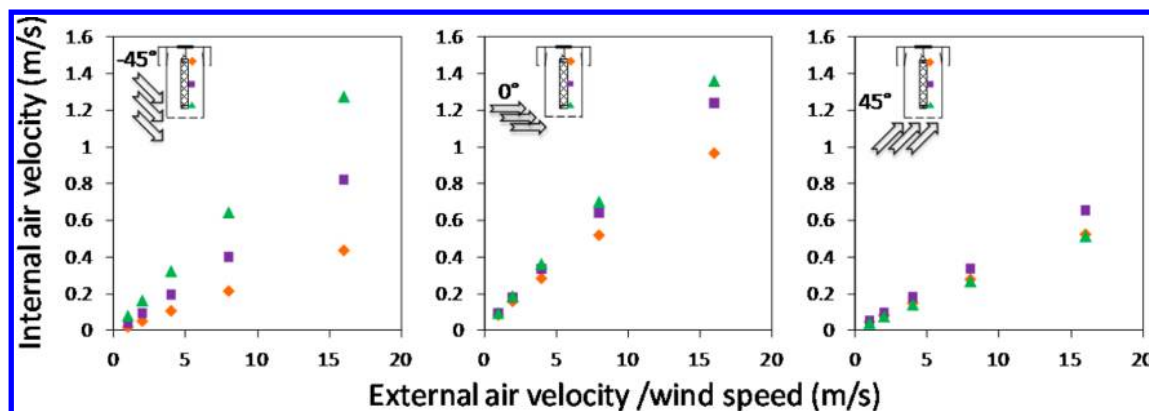
Figure 3. Variations of air velocities at three cross sections within the passive air sampler with ambient wind speed and angle obtained with computational fluid dynamics simulations. The top, middle, and bottom cross sections are represented by orange diamonds, purple squares, and green triangles. The internal air velocity at each cross section was the average of the four points shown in SI Figure S6.
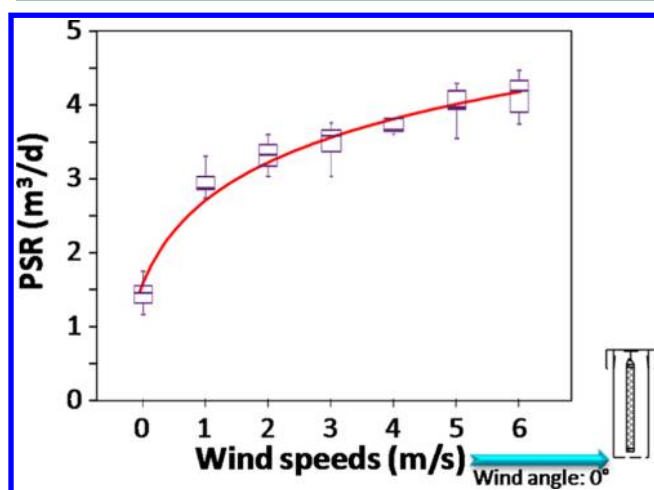
Figure 4. Passive air sampling rates derived from the kinetics of water vapor uptake from air by silica-gel at wind speeds of 0, 1, 2, 3, 4, 5, 6 m/s. The box-whiskers are based on five replicates. The red line is the logarithmic fit of eq 1.

lower wind speed can explain the relatively poor reproducibility noted above for the XAD-PAS (42%) under the quasi wind-still conditions compared to the ones under windy conditions (17 and 22%). While it is challenging to precisely replicate wind speed around a set of 12 passive air samplers under any wind condition, small differences in air flow around the samplers will cause a much larger uncertainty at lower wind speed because of the higher sensitivity of PSR to wind speed at low wind speeds. Duplicates under wind still conditions are therefore expected to yield widely different results even if they were exposed to only slightly different air flow velocities.

Comparing Uptake of PCBs in XAD and Water in Silica Gel. At wind-still conditions, the PSRs based on water uptake by silica-gel were 1.2−1.7 m³/d, which was comparable to previous water uptake experiments[32] but ~3 times higher than 2 × PSRs (multiplied by two to account for the 2-fold difference in the lengths of the sampling media) for PCB uptake by XAD. At 4 m/s, that is, the wind speed for the PCB uptake experiments, PSRs for water (3.6−3.8 m³/d) were ~1.5−3.5 times higher than the 2 × PSRs for PCB. Although such differences can be caused by the underestimation of PCBs concentrations in air sampled with HVS (discussed in the SI), a similar difference between passive sampling of water and PCBs

has been observed in a previous study which used a low volume air sampler to monitor air concentrations during the entire passive sampling period.[32] Such differences can be explained by differences in molecular diffusivity and sampling medium-side kinetic resistance between water and PCBs. Comparing the wind enhancement factors eliminates these factors confounding PSRs; the $WEF_{4:0}$ for the water uptake experiment (2.1−2.7) were statistically smaller than the $WEF_{4:0}$ of 2.5−3.5 derived from the PCB uptake experiment. Different approaches for generating wind in the two experiments (Figure 1a and b) are one possible explanation. Another may lie in the difference between chemicals and sampling media. Wind presumably affects mostly the air-side kinetic resistance. The effect of wind on PSR may depend on the relative contribution of the air-side resistance to the overall resistance, and therefore be different for different chemicals taken up by different sampling media.

Effect of Wind Speed on PSRs Based on CFD Simulations and Passive Air Sampling Model. From the simulated wind field at cross sections at the bottom, middle, and top of the PAS (Figure 3 and SI Figure S6), simulated wind speeds were over 70% lower inside than outside the housing, reflecting the housing's shielding of the sampling medium from the wind. This is consistent with a previous study showing that a sampler housing dampens the wind and PSR variability in PUF-PAS.[14] However, the shielding effect is much larger than for the double-bowl housing: In the latter, the internal wind speed reached 1 m/s when the ambient wind is 3.5 m/s,[14] while the wind speed inside the cylindrical housing only reached 1 m/s when the ambient wind is over 15 m/s. (Figure 3) CFD simulations conducted at different ambient wind speeds ($v_{ambient}$, m/s) indicated that they were linearly proportional to the wind speeds around the sampling medium within the sampler housing (v_{in}, m/s), that is, $v_{in} \propto v_{ambient}$ (Figure 3). This relationship together with the relationship between the thickness of the stagnant boundary layer surrounding a cylinder (δ, m) and v_{in},[34] and the relationship between the mass transfer coefficient of a chemical crossing the boundary layer (k_A, m/d) and δ enables us to derive (see SI for details) $k_A \propto v_{ambient}^{0.5}$. If the PSR were only determined by the kinetic resistance to diffusion through a boundary layer (i.e., PSR = $k_A A$, where A is the interfacial transfer area between the sampling medium and air), which was assumed by the widely adopted passive air sampling theory,[28,35,36] we should have observed PSR $\propto v_{ambient}^{0.5}$ or ln PSR = 0.5 ln $v_{ambient}$ + Const. However, linearly fitting of ln PSR with ln $v_{ambient}$ from the experiments (SI Figure S7) resulted in

$$\ln(\text{PSR/m}^3 \cdot \text{day}^{-1}) = 0.184(\pm 0.020)\ln(v_{\text{ambient}}/\text{m}\cdot\text{s}^{-1})$$
$$+ 1.068(\pm 0.025), R^2 = 0.75 \qquad (2)$$

Statistical test on the regression coefficient by ANCOVA (see SI) indicates that the empirically derived slope of 0.184 is significantly different ($p = 3.1 \times 10^{-6}$) from 0.5 and the variation of PSR with wind speed cannot be fully explained by the variation of the kinetic resistance within the stagnant boundary layer. This result thus complements our earlier studies[20,21] by indicating that the kinetic resistance posed by the stagnant boundary layer surrounding the sampling medium is not the dominant factor controlling the PSR.

Effect of Wind Angle on Uptake in Cylindrical Passive Sampler. *Effect of Wind Angle on PCB Uptake by XAD and on Water Uptake by Silica-Gel.* When the wind blew at the PAS at a 45° angle, the PSRs for PCBs were slightly higher (0.49−1.35 m³/d) than when the wind blew perpendicularly at the PAS (0.44−1.16 m³/d) (SI Table S5). The WEF$_{4:0}$ for the slanted PAS was 3.8 ± 0.2 compared to 3.3 ± 0.2 reported above for perpendicular wind. However, the differences in the PSRs were not significant for the majority of PCBs congeners (ANCOVA, see SI for detailed testing approach, SI Figure S8). While the experiment above only tested two different angles of wind relative to the PASs, variations of PSRs at additional angles (0°, ± 15° ± 30° and ±45°) were measured using the uptake of water in silica-gel. The average PSR observed at an angle of 0° (3.4 m³/d) was 10% lower than the PSRs observed at other angles (4.0 m³/d) (Figure 5). However, except between 0° and 15°, the PSRs at different angles were not
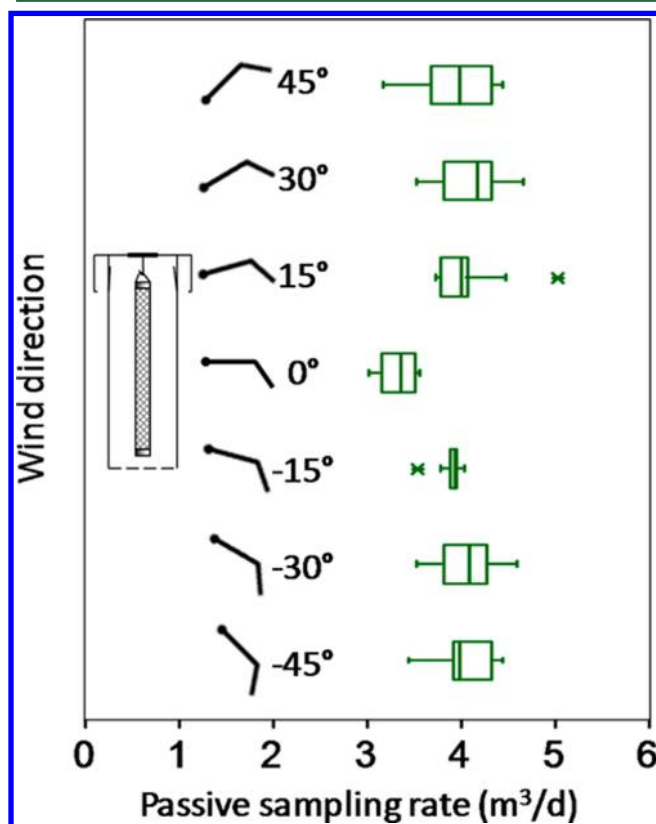
significantly different from each other (one-way ANOVA with Turkey posthoc multiple comparisons, SI Table S6).

Observations in this study suggest that the angle of wind incidence has little effect on the chemical uptake kinetics of the cylindrical PAS. In the field, PASs oftentimes are subject to highly variable wind conditions due to local turbulence or the effect of local terrain such as a mountain slope. A lack of influence of such variations on PSRs would assist in increasing the precision of the measurement.

Effect of Wind Angle on PSRs Based on CFD Simulations. Wind fields inside PASs subjected to ambient wind of different angles were simulated using CFD. In the PAS with wind blowing at 0°, higher wind speeds were simulated at the cross section closer to the opening (Figure 3 and SI Figure S9). The same pattern was simulated when the wind was blowing at a −45° angle, but wind speed differences at the three cross sections were larger. When the ambient wind was at a 45° angle, the simulated air velocities within the housing were lower than with wind at 0°. The air velocity at the middle cross section was higher than at the bottom and top. Similar patterns were simulated for wind angles between 0° and 90° (SI Figure S9); as the wind angle increased from 0° to 90°, the air velocity within the PAS decreased, which is mainly due to a decreased air velocity around the part of the sampling medium facing the wind (point a in SI Figure S9). The more directly the wind faces the opening of the PAS housing, the less it is able to enter it.

Whereas the CFD simulations predict variations of the air velocities surrounding the sampling medium with changing wind angles, the PCB and water uptake experiments showed no significant differences in the PSRs at different angles. We believe this is because the predicted variations in internal air velocity with wind angle lead to variations in PSR that are too small to observe experimentally. Since PSR $\propto v_{\text{ambient}}^{0.184}$ (eq 1) and $v_{\text{in}} \propto v_{\text{ambient}}$ (Figure 3), we expect PSR $\propto v_{\text{in}}^{0.184}$. A variation of v_{in} by ∼60% between wind angles of 0° and 45° is predicted to result in a change in PSR by ∼9%, which is too small to be observed if experimental variation is on the order of ∼10%.

Comparison of the Effect of Wind on Different Types of PAS. The effect of wind on the PSRs of the semienclosed cylindrical PAS[28] observed here is different from the effect of wind on the double-bowl PUF-PAS. First, the effect of wind speed and angle is smaller for the cylindrical PAS than for the double-bowl PAS. For example, a WEF$_{6:0}$ for water vapor of 2.6−3.1 reported here contrasts with a ∼7-fold increase in PSRs observed for the PUF-PAS at an ambient wind speed of ∼6 m/s compared to wind-still conditions.[14] Similarly, while a previous study showed a significant influence of the angle of wind incidence on PSRs of PUF-PAS,[25] the PSRs of the cylindrical PAS were largely unaffected by the angle of the wind.

The relationship between the PSR and wind speed is also very different. While here the PSR is more sensitive to wind speeds below 1 m/s, Tuduri et al.[14] suggested ambient wind below 3.5 m/s had no significant effect on the PSR in PUF-PAS. On the other hand, Tuduri et al.[14] observed a stronger wind dependence of the PSRs of the PUF-PAS at high equivalent ambient wind speeds: an increase from 4 to 7 m/s caused the PSRs for the double-bowl PUF-PAS to increase more than 4-fold (from <10 to ∼40 m³/d).[14] Based on water uptake by silica-gel as a surrogate, we only recorded a 30% increase in the PSRs of the cylindrical PAS as wind speed increased from 1 to 6 m/s.

Figure 5. Passive sampling rates based on water uptake by silica-gel when wind was blowing from different directions toward the sampler.

These differences are supported by a study[37] that compared XAD-PAS with PUF-PAS deployed side by side at multiple locations with different wind conditions around the globe and found XAD-PASs are much less influenced by wind than PUF-PASs. The larger wind speed dependence of the PUF-PAS is likely caused by the double-bowl design allowing wind to pass through the housing. The semienclosed cylindrical housing seems to be a much better buffer on the influence of ambient wind on PSRs, which results in more consistent PSRs at different sampling sites with different wind conditions. Furthermore, wind passing through the double bowl housing causes particles to be trapped in the PUF disk, which has been commonly observed.

We believe the slightly higher PSRs reported for the PUF-PAS compared to the XAD-PAS are also a result of wind penetrating the double bowl housing more easily.[22] If the lower end of the deployment length is limited by a chemical's detection limit, a higher PSR allows for shorter PAS deployments. However, the higher PSRs of the PUF-PAS come at the expense of much higher wind dependence of the PSRs. This high wind dependence of the PSRs of the PUF-PAS explains the need to deploy depuration compounds to avoid introducing large uncertainty to PUF-PAS-derived air concentrations.

Effect of Wind Speed on Passive Sampling Kinetics of Modified PAS Designs. As the comparison between double-bowl and cylindrical PASs showed that different housings can vary in how effectively they buffer wind, we explored whether design modifications can further reduce the influence of wind on the PSRs of the cylindrical PAS. Finer perforated bottom openings compared to the original design A used in designs B, C, and D lowered PSRs under windy and wind-still conditions (SI Figure S10a) by about the same extent, which is indicated by similar wind enhancement factors $WEF_{4:0}$ (SI Figure S10b). Reducing the area of the sampler housing opening in designs E and F, lowered the PSRs of design D under both windy and wind-still conditions to the same extent so that $WEF_{4:0}$ remained unchanged. With a better shielded sampling medium, designs G and H reduced PSRs for both windy and wind-still conditions but still could not reduce the wind influence. Interestingly, wrapping the outer mesh cylinder with tissue paper (design H) did not change the PSR compared to design G. Design I was subjected to even more pronounced wind influence than the other designs with $WEF_{4:0}$ being higher than in any of the other designs.

As the first study to test the influence of wind on the PSRs for different designs of PAS, the experiments suggest that while the modifications can reduce the PSRs of the cylindrical PAS housing, they have little effect on wind enhancement factors. Formulated positively, the experiments suggest that the current cylindrical housing is already as good at buffering the wind as can reasonably be expected. A lower wind speed dependence could likely be achieved by employing a relatively restrictive porous diffusion barrier, such as the one applied in Radiello type samplers, which can achieve $WEF_{4:0}$ as low as 1.1[24] and 1.3.[25] However, such a barrier not only would lower PSR by as much as an order of magnitude ($\sim$0.1 m^3/d), but would also raise concerns of sorption losses to the barrier material.

Implications. When deployed outdoors, variations in wind speed and angle between sites add uncertainty to the results of air concentrations measured with XAD-PAS. Based on the variation of PSRs with wind speed derived from water uptake experiments and the difference in the WEF between water and

SVOCs, such uncertainty would generally be within a factor of 2 (and when avoiding sites with extremely high or low wind speeds[29,30]). When such uncertainty is not acceptable, that is, when relative concentration differences smaller than this need to be discerned, one could seek to account for differences in wind exposure: If wind speeds are available for the deployment sites, a relationship similar to eq 1 could be used to scale compound-specific sampling rates. If no wind data are available, the normalization technique based on a SVOC with presumed uniform air concentrations described in Liu et al.[29] and Shunthirasingham et al.[30] can be employed. The strong dependence of PSRs on wind speed at low wind speeds means that PSRs for the XAD-PAS obtained in outdoor calibration studies are not necessarily valid indoors.

■ ASSOCIATED CONTENT

Ⓢ Supporting Information
Further information on experimental setup, instrumental parameters, data analysis, results and discussion. This material is available free of charge via the Internet at http://pubs.acs.org.

■ AUTHOR INFORMATION

Corresponding Author
*Phone: 416-287-7225; e-mail: frank.wania@utoronto.ca.
Notes
The authors declare no competing financial interest.

■ REFERENCES

(1) Li, Y. M.; Geng, D. W.; Liu, F. B.; Wang, T.; Wang, P.; Zhang, Q. H.; Jiang, G. B. Study of PCBs and PBDEs in King George Island, Antarctica, using PUF passive air sampling. *Atmos. Environ.* **2012**, *51*, 140−145.

(2) Chakraborty, P.; Zhang, G.; Li, J.; Xu, Y.; Liu, X.; Tanabe, S.; Jones, K. C. Selected organochlorine pesticides in the atmosphere of major Indian cities: Levels, regional versus local variations, and sources. *Environ. Sci. Technol.* **2010**, *44*, 8038−8043.

(3) United Nations. Environment Programme. Stockholm Convention on persistent organic pollutants (POPs). http://chm.pops.int/Convention/ (accessed April 2012).

(4) Shunthirasingham, C.; Oyiliagu, C. E.; Cao, X. S.; Gouin, T.; Wania, F.; Lee, S.-C.; Pozo, K.; Harner, T.; Muir, D. C. G. Spatial and temporal pattern of pesticides in the global atmosphere. *J. Environ. Monitor.* **2010**, *12*, 1650−1657.

(5) Liu, S. Z.; Tao, S.; Liu, W. X.; Dou, H.; Liu, Y. N.; Zhao, J. Y.; Little, M. G.; Tian, Z. F.; Wang, J. F.; Wang, L. G.; Gao, Y. Seasonal and spatial occurrence and distribution of atmospheric polycyclic aromatic hydrocarbons (PAHs) in rural and urban areas of the North Chinese Plain. *Environ. Pollut.* **2008**, *156*, 651−656.

(6) Li, Y. M.; Zhang, Q. H.; Ji, D. S.; Wang, T.; Wang, Y. W.; Wang, P.; Ding, L.; Jiang, G. B. Levels and vertical distributions of PCBs, PBDEs, and OCPs in the atmospheric boundary layer: Observation from the Beijing 325 m meteorological tower. *Environ. Sci. Technol.* **2009**, *43*, 1030−1035.

(7) Zhang, G.; Chakraborty, P.; Li, J.; Sampathkumar, P.; Balasubramanian, T.; Kathiresan, K.; Takahashi, S.; Subramanian, A.;

Tanabe, S.; Jones, K. C. Passive atmospheric sampling of organo-chlorine pesticides, polychlorinated biphenyls, and polybrominated diphenyl ethers in urban, rural, and wetland sites along the coastal length of India. *Environ. Sci. Technol.* **2008**, *42*, 8218−8223.

(8) Bohlin, P.; Jones, K. C.; Strandberg, B. Field evaluation of polyurethane foam passive air samplers to assess airborne PAHs in occupational environments. *Environ. Sci. Technol.* **2009**, *44*, 749−754.

(9) Abdallah, M. A. E.; Harrad, S. Modification and calibration of a passive air sampler for monitoring vapor and particulate phase brominated flame retardants in indoor air: Application to car interiors. *Environ. Sci. Technol.* **2010**, *44*, 3059−3065.

(10) Zhang, X. M.; Diamond, M. L.; Robson, M.; Harrad, S. Sources, emissions, and fate of polybrominated diphenyl ethers and polychlorinated biphenyls indoors in Toronto, Canada. *Environ. Sci. Technol.* **2011**, *45*, 3268−3274.

(11) Li, X. M.; Li, Y. M.; Zhang, Q. H.; Wang, P.; Yang, H. B.; Jiang, G. B.; Wei, F. S. Evaluation of atmospheric sources of PCDD/Fs, PCBs and PBDEs around a steel industrial complex in northeast China using passive air samplers. *Chemosphere* **2011**, *84*, 957−963.

(12) Baldwin, P. E. J.; Maynard, A. D. A survey of wind speeds in indoor workplaces. *Ann. Occup. Hyg.* **1998**, *42*, 303−313.

(13) Bornstein, R. D.; Johnson, D. S. Urban-rural wind velocity differences. *Atmos. Environ.* **1977**, *11*, 597−604.

(14) Tuduri, L.; Harner, T.; Hung, H. Polyurethane foam (PUF) disks passive air samplers: Wind effect on sampling rates. *Environ. Pollut.* **2006**, *144*, 377−383.

(15) Moeckel, C.; Harner, T.; Nizzetto, L.; Strandberg, B.; Lindroth, A.; Jones, K. C. Use of depuration compounds in passive air samplers: Results from active sampling-supported field deployment, potential uses, and recommendations. *Environ. Sci. Technol.* **2009**, *43*, 3227−3232.

(16) Thomas, J.; Holsen, T. M.; Dhaniyala, S. Computational fluid dynamic modeling of two passive samplers. *Environ. Pollut.* **2006**, *144*, 384−392.

(17) Harner, T.; Shoeib, M.; Diamond, M.; Stern, G.; Rosenberg, B. Using passive air samplers to assess urban−rural trends for persistent organic pollutants. 1. Polychlorinated biphenyls and organochlorine pesticides. *Environ. Sci. Technol.* **2004**, *38*, 4474−4483.

(18) Klánová, J.; Èupr, P.; Kohoutek, J.; Harner, T. Assessing the influence of meteorological parameters on the performance of polyurethane foam-based passive air samplers. *Environ. Sci. Technol.* **2008**, *42*, 550−555.

(19) Melymuk, L.; Robson, M.; Helm, P. A.; Diamond, M. L. Evaluation of passive air sampler calibrations: Selection of sampling rates and implications for the measurement of persistent organic pollutants in air. *Atmos. Environ.* **2011**, *45*, 1867−1875.

(20) Zhang, X. M.; Tsurukawa, M.; Nakano, T.; Lei, Y. D.; Wania, F. Sampling medium side resistance to uptake of semivolatile organic compounds in passive air samplers. *Environ. Sci. Technol.* **2011**, *45*, 10509−10515.

(21) Zhang, X. M.; Wania, F. Modeling the uptake of semivolatile organic compounds by passive air samplers: Importance of mass transfer processes within the porous sampling media. *Environ. Sci. Technol.* **2012**, *46*, 9563−9570.

(22) Skov, H.; Sørensen, B. T.; Landis, M. S.; Johnson, M. S.; Sacco, P.; Goodsite, M. E.; Lohse, C.; Christiansen, K. S. Performance of a new diffusive sampler for Hg-0 determination in the troposphere. *Environ. Chem.* **2007**, *4*, 75−80.

(23) Pennequin-Cardinal, A.; Plaisance, H.; Locoge, N.; Ramalho, O.; Kirchner, S.; Galloo, J. C. Performances of the Radiello® diffusive sampler for BTEX measurements: Influence of environmental conditions and determination of modelled sampling rates. *Atmos. Environ.* **2005**, *39*, 2535−2544.

(24) Tao, S.; Liu, Y.; Xu, W.; Lang, C.; Liu, S.; Dou, H.; Liu, W. Calibration of a passive sampler for both gaseous and particulate phase polycyclic aromatic hydrocarbons. *Environ. Sci. Technol.* **2007**, *41*, 568−73.

(25) May, A. A.; Ashman, P.; Huang, J.; Dhaniyala, S.; Holsen, T. M. Evaluation of the polyurethane foam (PUF) disk passive air sampler: Computational modeling and experimental measurements. *Atmos. Environ.* **2011**, *45*, 4354−4359.

(26) Söderström, H. S.; Bergqvist, P. A. Wind effects on passive air sampling of PAHs and PCBs. *Bull. Environ. Contam. Toxicol.* **2005**, *74*, 429−436.

(27) Söderström, H. S.; Bergqvist, P. A. Passive air sampling using semipermeable membrane devices at different wind-speeds in situ calibrated by performance reference compounds. *Environ. Sci. Technol.* **2004**, *38*, 4828−4834.

(28) Wania, F.; Shen, L.; Lei, Y. D.; Teixeira, C.; Muir, D. C. G. Development and calibration of a resin-based passive sampling system for monitoring persistent organic pollutants in the atmosphere. *Environ. Sci. Technol.* **2003**, *37*, 1352−1359.

(29) Liu, W. J.; Chen, D. Z.; Liu, X. D.; Zheng, X. Y.; Yang, W.; Westgate, J. N.; Wania, F. Transport of semivolatile organic compounds to the Tibetan Plateau: spatial and temporal variation in air concentrations in mountainous western Sichuan, China. *Environ. Sci. Technol.* **2010**, *44*, 1559−1565.

(30) Shunthirasingham, C.; Barra, R.; Mendoza, G.; Montory, M.; Oyiliagu, C. E.; Lei, Y. D.; Wania, F. Spatial variability of atmospheric semivolatile organic compounds in Chile. *Atmos. Environ.* **2011**, *45*, 303−309.

(31) Daly, G. L.; Lei, Y. D.; Teixeira, C.; Muir, D. C. G.; Wania, F. Pesticides in western Canadian mountain air and soil. *Environ. Sci. Technol.* **2007**, *41*, 6020−6025.

(32) Zhang, X. M.; Wong, C.; Lei, Y. D.; Wania, F. Influence of sampler configuration on the uptake kinetics of a passive air sampler. *Environ. Sci. Technol.* **2012**, *46*, 397−403.

(33) Gouin, T.; Wania, F.; Ruepert, C.; Castillo, L. E. Field testing passive air samplers for current use pesticides in a tropical environment. *Environ. Sci. Technol.* **2008**, *42*, 6625−6630.

(34) Nobel, P. S. Boundary-layers of air adjacent to cylinders—Estimation of effective thickness and measurements on plant material. *Plant Physiol.* **1974**, *54*, 177−181.

(35) Bartkow, M. E.; Booij, K.; Kennedy, K. E.; Müller, J. F.; Hawker, D. W. Passive air sampling theory for semivolatile organic compounds. *Chemosphere* **2005**, *60*, 170−176.

(36) Shoeib, M.; Harner, T. Characterization and comparison of three passive air samplers for persistent organic pollutants. *Environ. Sci. Technol.* **2002**, *36*, 4142−4151.

(37) Shunthirasingham, C. *Pesticide fate in different climates.* PhD Thesis, Department of Chemistry, University of Toronto, 2010.

Supporting Information

Effect of Wind on the Chemical Uptake Kinetics of a Passive Air Sampler

Xianming Zhang,[†] Trevor N. Brown,[†] Amer Ansari,[†] Beom Yeun,[†] Ken Kitaoka,[‡] Akira Kondo,[‡]

*Ying D. Lei,[†] Frank Wania[† *]*

[†] Department of Chemistry and Department of Physical and Environmental Sciences, University

of Toronto Scarborough, Toronto, Ontario M1C 1A4, Canada

[‡] Osaka University, Graduate School of Engineering, 2-1, Yamadaoka, Suita 565-0871, Japan

* Corresponding author phone: 416-287-7225; email: frank.wania@utoronto.ca

[†] University of Toronto Scarborough

[‡] Osaka University

Table of Contents

Figure S1. Experimental setup to study potential wind effects on PCB uptake by the XAD passive air sampler. The passive air samplers on the left and on the right were subjected to wind blowing at 0° angle and 45° angle respectively.
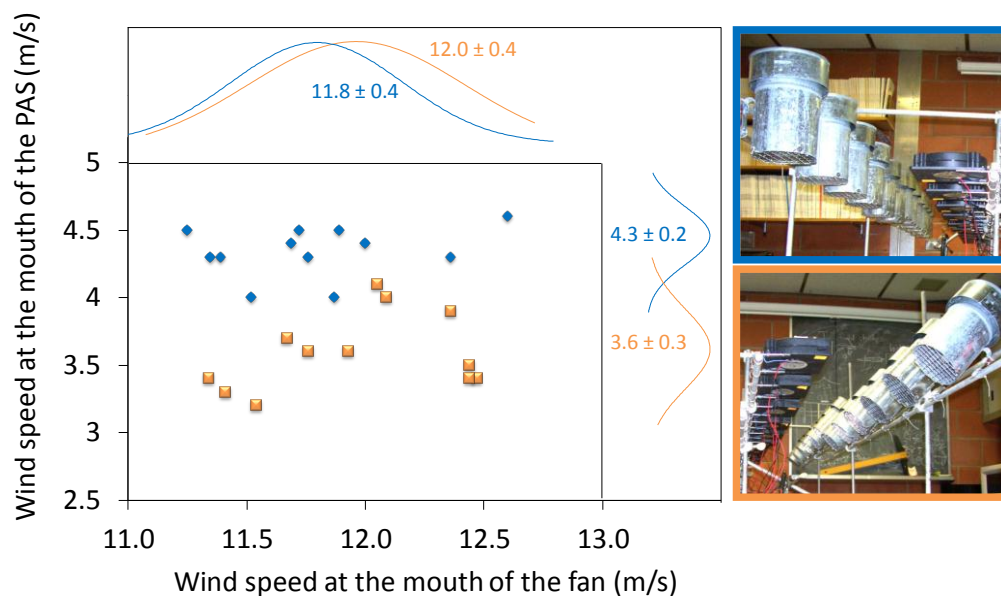
Figure S2. Variations of wind speed measured at the mouth of the fans (point A of Figure 1a) and at the openings of the sampler housings (point B of Figure 1a) for the 24 passive air samplers subjected to lab-generated windy conditions.
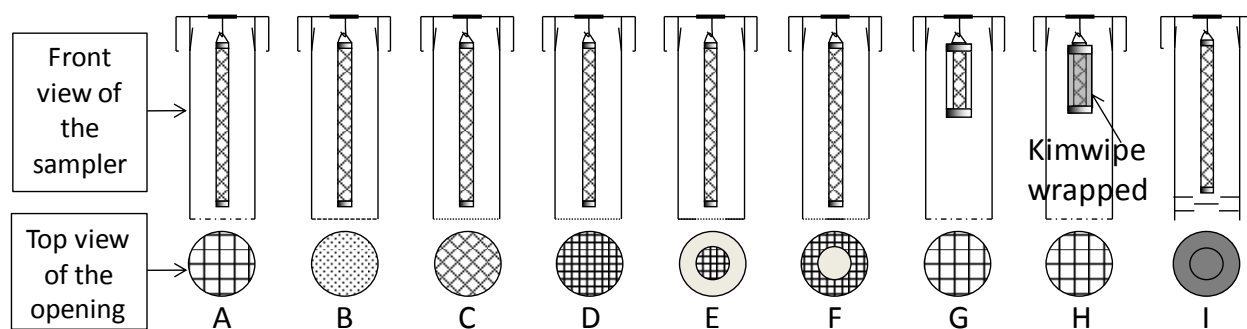
Figure S3. Modifications of cylindrical passive air samplers for testing the influence of wind on the passive sampling rate.

Table S1. Modifications on the opening of the housing of the cylindrical passive air sampler

Modification	Total area (cm^2)	Shape of openings	Open area of each hole (cm^2)	Number of openings	Total opening area (cm^2)
B	65.6	Circle	0.01	894	8.9
C	65.6	Square	0.09	422	37.9
D	65.6	Oval	0.22	242	53.2
E	65.6		0.22	121	27
F	65.6		0.22	121	27

Sampling and extraction of gas- and particle-phase PCB in the air of the room, in which XAD-PAS were deployed under different laboratory-generated wind conditions

Three high volume (HiVol) air samples were collected at day 90, 121 and 140 in the room in which the XAD-PAS were deployed. During the sampling time of ~24 h, 391, 235, 246 m^3 were sampled respectively. The air was pulled through a glass fiber filter (GFF) to collect the particulate phase and then through a glass cartridge containing XAD-2 resin (Supelco, Supelpak-2, precleaned Amberlite XAD-2 resin, 20/ 60 mesh) placed between two layers of polyurethane foam (PUF) (Supelco, precleaned large PUF plug, 6 × 3.8 cm) to collect the vapor phase. The GFF had been baked at 450 °C overnight prior to use. After sampling, the cartridges and GFFs were wrapped in solvent-rinsed aluminum foil and sealed in Ziploc bags. All the HiVol samples and PAS were kept frozen until extraction and analysis.

The HiVol air samples were Soxhlet extracted with dichloromethane (DCM) for ~24 h. PUF-XAD-PUF sandwiches and GFF were extracted separately to determine the distribution of pesticides between gas and particle phase. The second PUF plugs of PUF-XAD-PUF sandwiches were extracted separately to quantify breakthrough. Prior to extraction, each sample was spiked with 100μL 250 pg/μL $^{13}C_{12}$-labeled PCB-77, -101, -141 and -178 (Cambridge Isotope) as surrogate standards to quantify recovery. The extract was roto-evaporated to ~2 mL and eluted through a disposable pasteur pipet packed with dehydrated sodium sulphate to remove moisture. The eluent was blown down with high purity N_2, solvent exchanged to iso-octane and reduced to ~0.5 mL in a GC vial, to which 100 ng mirex was added for volume correction.

PCBs measured in the second PUF plugs were less than 5% of the total amounts sampled by the PUF-XAD-PUF sandwiches, indicating negligible breakthrough of analytes during sampling. Recoveries of the four surrogate standards for the HiVol samples ranged between 67 and 116% with an interquatile range of 80-91%.

Concentrations of the most commonly detected PCB congeners in the atmospheric gas and particle phase are listed in Table S3. The particle-bound PCBs accounted for less than 3% of PCBs in bulk air. While samples 2 and 3 had very similar concentrations (within 3 to 23 % depending on the congener), those in sample 1 were generally two-fold higher (Table S3). Because we expect indoor air concentrations to vary less than a factor of two, we treated sample 1 as an outlier and used the average gas phase concentration of samples 2 and 3 for the passive air sampler calibration.

While continuous active sampling for the entire length of passive air sampler deployment (5 month in the present case) would be ideal for a PAS calibration, most such calibrations only sample for a fraction of the time. A lower number of simultaneously collected active samples is defensible in an indoor setting with lower variability in PCB air concentration than outdoors. We recognize that the variability between the air concentrations of the three HiVol samples was larger than expected and in retrospect we would have preferred to have a larger number of active samples. Due to these uncertainties in the air concentrations, we suggest to be cautious when comparing the PSRs derived in this study with others. However, these uncertainties do not affect the main conclusions of this study regarding the influence of wind on chemical uptake kinetics. This study focused on ratios of PSRs under different wind conditions, which are entirely independent of the air concentrations.

Table S2. Target ions, qualifier ions and limit of detection (LOD) of the PCB homolog groups analyzed using GC-MS selected ion monitoring mode.

Class	Chemical	Target Ion	Qualifier Ion	(Qual./Targ.) *100%	LOD [a] (ng/sample)
Internal Standard	Mirex	272	274	81.1	n/a
Surrogate Standard	^{13}CPCB77	304	302	77.2	n/a
Surrogate Standard	^{13}CPCB101	338	340	64.8	n/a
Surrogate Standard	^{13}CPCB141	372	374	81	n/a
Surrogate Standard	^{13}CPCB178	406	408	97.2	n/a
Target Analyte	Tri-CB	256	258	98	0.5
Target Analyte	Tetra-CB	292	290	76.7	1
Target Analyte	Penta-CB	326	328	65.3	0.2
Target Analyte	Hexa-CB	360	362	81.4	1.5

[a] LOD calculated as the chemical amount of which the instrument detects a signal corresponding to three times of the noise level.

Table S3. Air concentrations of the most commonly detected PCB congeners in the gas and particle phase measured using high volume air samplers

PCB Congener	particle phase (ng/m^3) sample			gas phase (ng/m^3) sample			bulk (ng/m^3) sample			particle-bound fraction sample		
	1	2	3	1	2	3	1	2	3	1	2	3
TriCB31/28	0.02	0.04	0.04	6.83	3.37	4.09	6.86	3.41	4.13	0.3%	1.3%	1.0%
TetraCB52	0.03	0.12	0.03	49.8	24.0	28.1	49.8	24.1	28.1	0.1%	0.5%	0.1%
TetraCB49	0.02	0.05	0.03	12.9	6.72	6.96	12.9	6.77	6.99	0.1%	0.7%	0.4%
TetraCB44	0.02	0.07	0.03	20.2	10.0	11.5	20.2	10.1	11.6	0.1%	0.7%	0.2%
TetraCB74	0.01	0.03	0.02	8.27	3.21	3.78	8.29	3.24	3.80	0.1%	1.1%	0.4%
TetraCB66	0.02	0.05	0.02	8.42	3.76	4.15	8.44	3.81	4.18	0.2%	1.3%	0.6%
PentaCB95	0.03	0.15	0.02	47.5	21.8	24.7	47.5	21.9	24.7	0.1%	0.7%	0.1%
PentaCB101	0.07	0.24	0.04	67.3	29.2	32.5	67.3	29.5	32.6	0.1%	0.8%	0.1%
PentaCB99	0.03	0.08	0.03	21.5	9.14	10.1	21.5	9.22	10.1	0.1%	0.9%	0.3%
PentaCB87	0.05	0.15	0.04	35.1	14.8	11.8	35.2	14.9	11.9	0.2%	1.0%	0.3%
PentaCB110	0.10	0.23	0.06	51.4	20.8	22.8	51.5	21.0	22.8	0.2%	1.1%	0.3%
PentaCB118	0.07	0.12	0.04	23.5	8.78	9.48	23.6	8.89	9.53	0.3%	1.3%	0.4%
HexaCB149	0.06	0.10	0.05	17.3	6.92	7.36	17.4	7.02	7.41	0.3%	1.4%	0.7%
HexaCB153	0.05	0.07	0.04	12.1	4.53	5.13	12.2	4.61	5.17	0.4%	1.6%	0.8%
HexaCB138	0.05	0.06	0.04	6.27	2.44	2.38	6.32	2.49	2.43	0.8%	2.3%	1.7%

Table S4. Amount (ng) of PCBs analyzed in the XAD-PASs at different deployment time

deployment time (d)	35	35	67	67	92	92	112	112	127	127	144	144
condition / PCB congener	Accumulated amount (ng)											
Windy, 0° Angle												
TriCB31/28	46	38	88	83	162	189	201	212	255	215	303	258
TetraCB52	435	354	838	783	1512	1773	1857	1925	2320	2039	2729	2262
TetraCB49	120	113	268	253	478	530	555	610	726	644	872	572
TetraCB44	160	135	305	300	570	656	684	723	858	771	1061	803
TetraCB74	89	73	166	164	248	352	385	398	484	415	564	492
PentaCB95	436	370	832	812	1525	1727	1884	1957	2366	2084	2829	2349
TetraCB66	94	78	179	167	330	398	403	435	504	447	614	498
PentaCB101	663	570	1202	1178	2214	2574	2813	2892	3273	3107	4169	3350
PentaCB99	167	144	306	304	548	660	715	743	870	782	1082	843
PentaCB87	297	248	546	529	986	1161	1253	1346	1557	1394	1852	1546
PentaCB110	554	462	1001	989	1873	2145	2344	2418	2874	2606	3494	2835
HexaCB149	181	155	316	319	583	669	740	769	918	838	1119	890
PentaCB118	319	266	496	552	928	1105	1241	1233	1508	1296	1951	1440
HexaCB153	160	128	295	277	530	636	671	723	763	675	1006	709
HexaCB138	90	79	154	158	284	338	377	368	439	409	528	446
Windy, 45° Angle												
TriCB31/28	39	42	98	89	176	150	186	192	184	231	266	208
TetraCB52	344	377	908	804	1743	1381	1657	1761	1695	2164	2382	1858
TetraCB49	99	121	285	252	483	453	434	513	509	592	731	591
TetraCB44	133	143	348	294	628	516	576	642	612	814	860	638
TetraCB74	74	78	186	165	332	258	350	348	340	434	499	381
PentaCB95	363	393	946	817	1694	1380	1702	1733	1697	2224	2382	1873
TetraCB66	80	78	207	180	347	307	367	377	358	461	489	402
PentaCB101	543	587	1361	1184	2439	2007	2489	2526	2460	3237	3044	2700
PentaCB99	137	147	348	304	628	515	648	654	626	813	843	677
PentaCB87	245	255	619	538	1085	900	1160	1118	1107	1472	1510	1218
PentaCB110	442	477	1151	986	2042	1677	2165	2101	2069	2695	2886	2234
HexaCB149	144	157	370	316	661	520	678	659	652	866	895	704
PentaCB118	252	269	558	557	960	879	1112	1174	1144	1318	1501	1228
HexaCB153	130	129	303	254	540	459	628	570	556	662	701	577
HexaCB138	67	78	177	155	322	252	335	322	303	416	423	342
Quasi wind-still												
TriCB31/28	11	13	20	56	22	38	45	78	51	71	79	74
TetraCB52	98	109	190	471	201	352	387	705	475	638	702	652
TetraCB49	32	36	61	154	59	109	120	226	151	193	213	211
TetraCB44	37	41	72	181	73	133	150	271	181	241	262	247
TetraCB74	20	22	37	97	39	72	80	142	97	125	137	131
PentaCB95	96	107	194	475	195	359	414	735	490	651	688	667
TetraCB66	22	25	37	109	42	79	85	164	98	138	155	128
PentaCB101	143	158	281	690	277	525	591	1064	718	939	994	954
PentaCB99	36	39	71	176	69	133	149	275	185	238	252	241
PentaCB87	64	66	123	309	121	236	264	495	310	428	455	423
PentaCB110	113	119	224	558	219	428	489	901	585	777	818	787
HexaCB149	38	41	73	181	71	140	156	286	191	247	264	249
PentaCB118	63	67	120	302	123	246	274	497	309	422	454	428
HexaCB153	31	35	63	151	56	107	135	250	157	191	189	213
HexaCB138	17	18	34	85	31	64	73	135	88	115	122	121

Derivation of passive sampling rate (PSR) from passive air sampler calibration

The principle and approach to derive PSR (m^3/d) from PAS calibration has been described in detail previously (e.g. Shoeib, M.; Harner, T. Characterization and comparison of three passive air samplers for persistent organic pollutants. *Environ. Sci. Technol.* **2002**, *36*, 4142-4151). Briefly, the PSR is derived based on the equation $m = PSR \cdot C_A \cdot t$, where m is the amount (normally in ng) of chemicals accumulated in the passive sampling medium during the PAS deployment time t (d). C_A (ng/m^3) is the concentration of the chemical in ambient air during the calibration of PAS and is determined by active air sampling. Often an equivalent sampled volume is defined as $V_{eq} = m/C_A = PSR \cdot t$. To reduce the influence of variability on the calibrated PSR and to ensure the chemical uptake is within the quasi-linear kinetics range, the calibration requires deploying multiple PASs over various lengths of deployment. V_{eq} can be plotted against the lengths of deployment and the slope of the linear regression line is the calibrated PSR (e.g. Figure 2).

$$|AB| = V_{eq,half-wind}(t) - V_{eq,no-wind}(t)$$
$$|BC| = |AB|$$
$$V_{eq,cont-wind}(t) = V_{eq,half-wind}(t) + |BC|$$
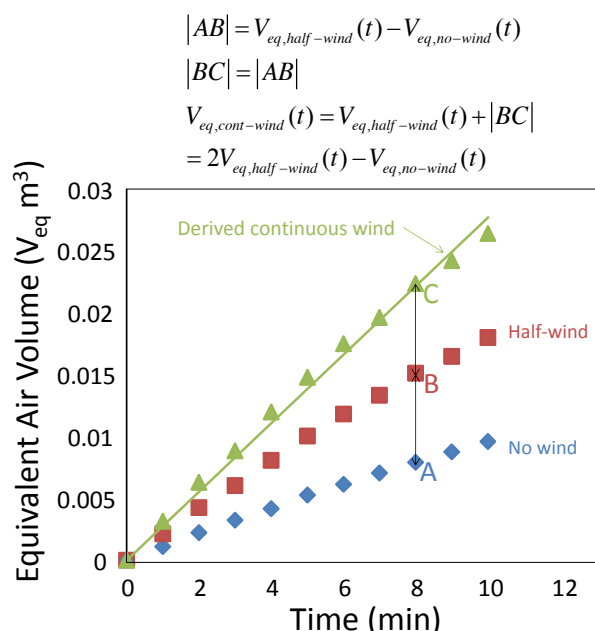$$= 2V_{eq,half-wind}(t) - V_{eq,no-wind}(t)$$

Figure S4. Derivation of the water uptake profile for continuous wind condition based on the uptake under half-wind and no-wind conditions.
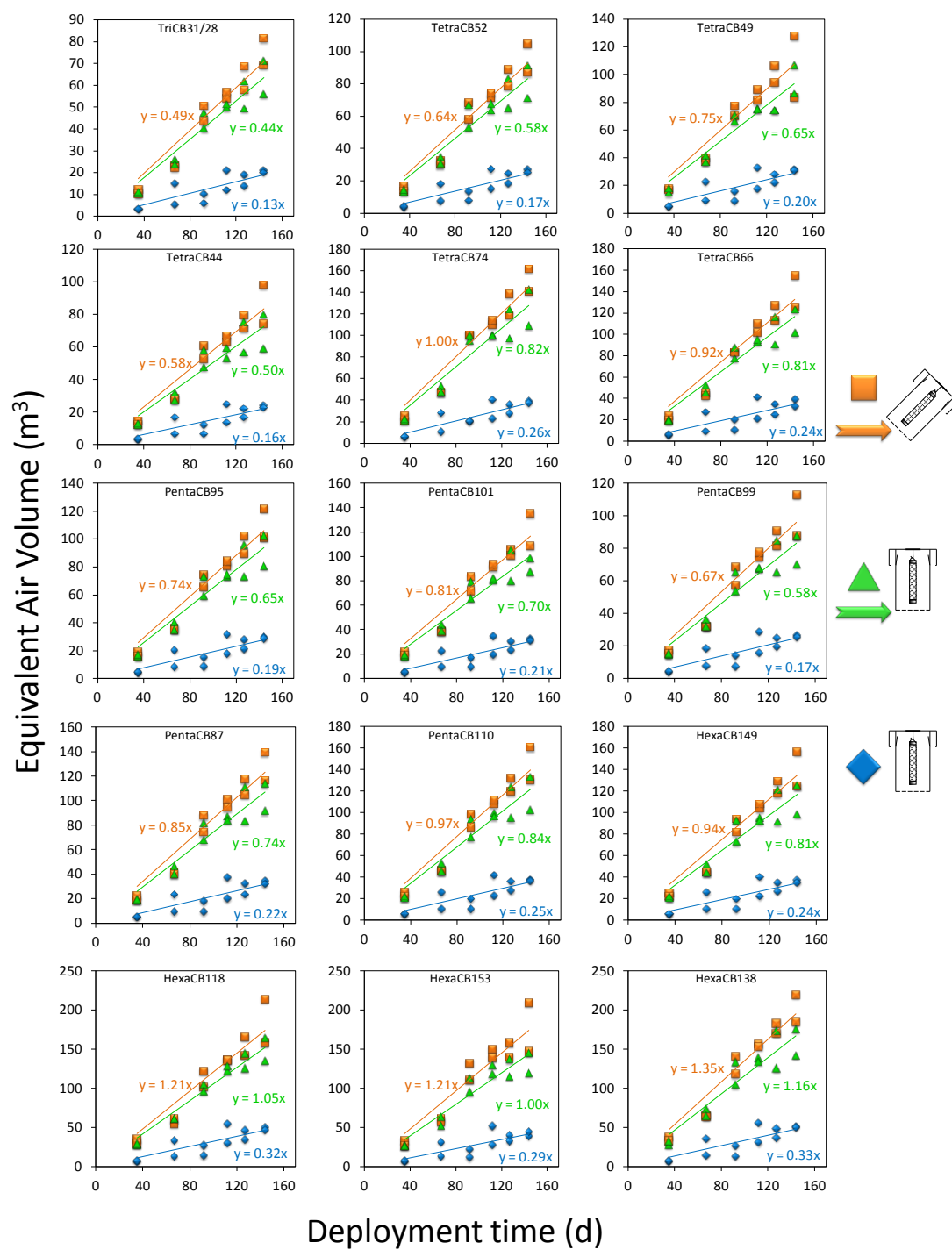
Figure S5. Passive air sampling kinetics for samplers under windy (lab generated wind blowing at 45° slanted angle and at straight angle towards the cylindrical passive air samplers) and wind still conditions.

Table S5. Passive sampling rates (PSRs) derived as the slopes of the regression[a] between the deployment time and equivalent sampling volume.

	Windy, 45° Angle			Windy, 0° Angle			quasi wind-still		
PCB congener	PSR (m^3/d)	SE[b]	R^{2} [c]	PSR (m^3/d)	SE	R^2	PSR (m^3/d)	SE	R^2
TriCB31/28	0.49	0.02	0.98	0.44	0.02	0.99	0.13	0.01	0.93
TetraCB52	0.64	0.02	0.99	0.58	0.02	0.98	0.17	0.01	0.94
TetraCB49	0.75	0.03	0.98	0.65	0.02	0.99	0.20	0.02	0.93
TetraCB44	0.58	0.02	0.98	0.50	0.02	0.98	0.16	0.01	0.93
TetraCB74	1.00	0.04	0.99	0.89	0.04	0.98	0.26	0.02	0.95
TetraCB66	0.92	0.03	0.99	0.81	0.03	0.99	0.24	0.02	0.92
PentaCB95	0.74	0.03	0.99	0.65	0.02	0.98	0.19	0.02	0.94
PentaCB101	0.81	0.03	0.99	0.70	0.03	0.99	0.21	0.02	0.94
PentaCB99	0.67	0.03	0.98	0.58	0.02	0.98	0.17	0.01	0.93
PentaCB87	0.85	0.03	0.99	0.74	0.03	0.98	0.22	0.02	0.93
PentaCB110	0.97	0.03	0.99	0.84	0.03	0.98	0.25	0.02	0.93
HexaCB149	0.94	0.03	0.99	0.81	0.03	0.98	0.24	0.02	0.93
PentaCB118	1.21	0.05	0.98	1.05	0.03	0.99	0.32	0.03	0.93
HexaCB153	1.21	0.05	0.98	1.00	0.04	0.98	0.29	0.03	0.92
HexaCB138	1.35	0.04	0.99	1.16	0.05	0.98	0.33	0.03	0.93

[a] regression forced through the origin

[b] Standard error of the regression coefficients (PSRs)

[c] For regression through the origin (the no-intercept model), R^2 measures the proportion of the variability in the dependent variable explained by regression. This cannot be compared to R^2 for models which include an intercept
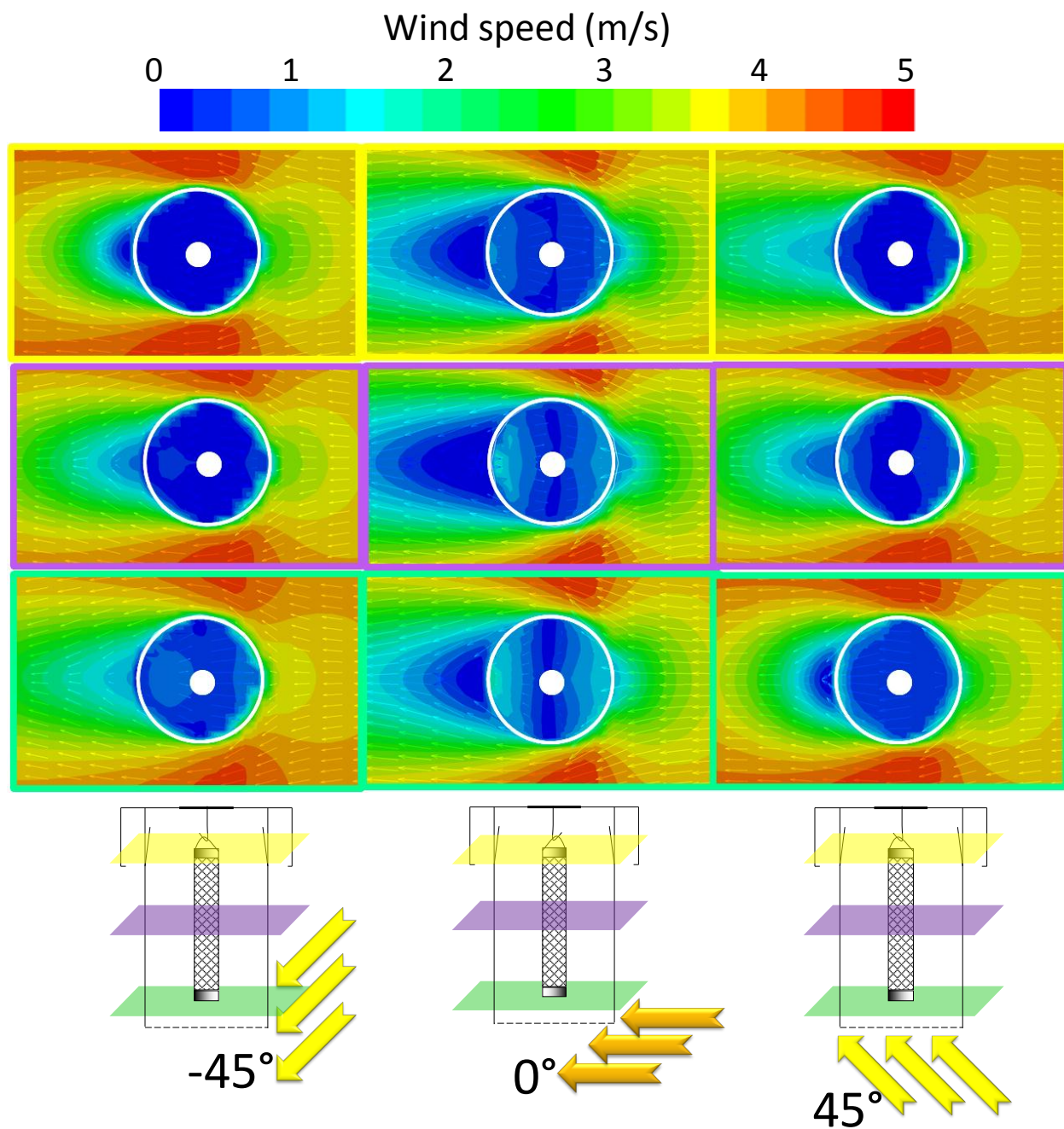
Figure S6. Computational fluid dynamic simulations of wind field on the cross sections at the top, middle and bottom of the XAD mesh cylinders within the housing of the passive air samplers subject to wind blowing at -45°, 0° and 45° angles towards the sampler.

Variations of the mass transfer coefficient (k_A) for a chemical to diffuse across the stagnant air boundary layer surrounding a cylindrical passive sampling medium with ambient wind speed.

Based on CFD simulations conducted at different ambient wind speeds, the wind speeds around the sampling medium within the sampler housing (v_{in}, m/s) were linearly proportional to the ambient wind speeds ($v_{ambient}$, m/s):

$$v_{in} \propto v_{ambient} \quad \text{(Equation S1)}$$

In the study by Nobel (Nobel, P. S. Boundary-layers of air adjacent to cylinders - estimation of effective thickness and measurements on plant material. *Plant Physiol*. **1974**, *54*, 177-181), the thickness (δ, m) of stagnant boundary layer surrounding a cylinder (diameter d in m) and the wind speed (v_{wind} in m/s, equivalent to the wind speed v_{in} within the sampler housing in this study) have the following relationship:

$$\delta(m) = 0.0074 d^{0.5} v_{wind}^{-0.5} = 0.0074 d^{0.5} v_{in}^{-0.5} \quad \text{(Equation S2)}$$

The mass transfer coefficient (k_A) for a chemical to diffuse across the stagnant air boundary layer is related to the molecular diffusivity of a chemical in air (D_A) and the thickness of stagnant air layer that diffusion occurs (δ, m):

$$k_A = D_A / \delta \quad \text{(Equation S3)}$$

Based on Equation S1-3, we can derive $k_A \propto v_{ambient}^{0.5}$.

Testing the slopes of linear regressions using analysis of covariance (ANCOVA).

ANCOVA Model: $Y_{ij} = \mu + A_i + \beta(X_{ij} - \bar{X}) + \varepsilon_{ij}$

Y_{ij}:   The value of the response variable for the jth observation in the ith treatment of factor A

μ: The overall mean value of the response variable

A_i: The effect of the ith treatment of factor A, defined as the difference of the mean of each A and the overall mean ($A_i = \mu_i - \mu$)

β: A combined regression coefficient representing the pooling of the regression slopes of Y on X within each group.

X_{ij}:   Covariate value for the jth replicated observation from the ith level of factor A

$\bar{X}$:   mean value of covariate

ε_{ij}:   Unexplained error associated with jth replicate observation from the ith level of factor A

Null hypothesis to test the slopes of regression lines (H_0): no difference between the regression coefficients under treatment of A_1, A_2…A_i (i.e. $\beta_1 = \beta_2 = ... = \beta_i$)

When the interaction effect between the treatment factor A and the covariate in the ANCOVA model is significant, the effect the covariate on the response depends on the treatment factor, which means the slopes of regressions for each treatment factor are not statistically the same and H_0 is rejected.
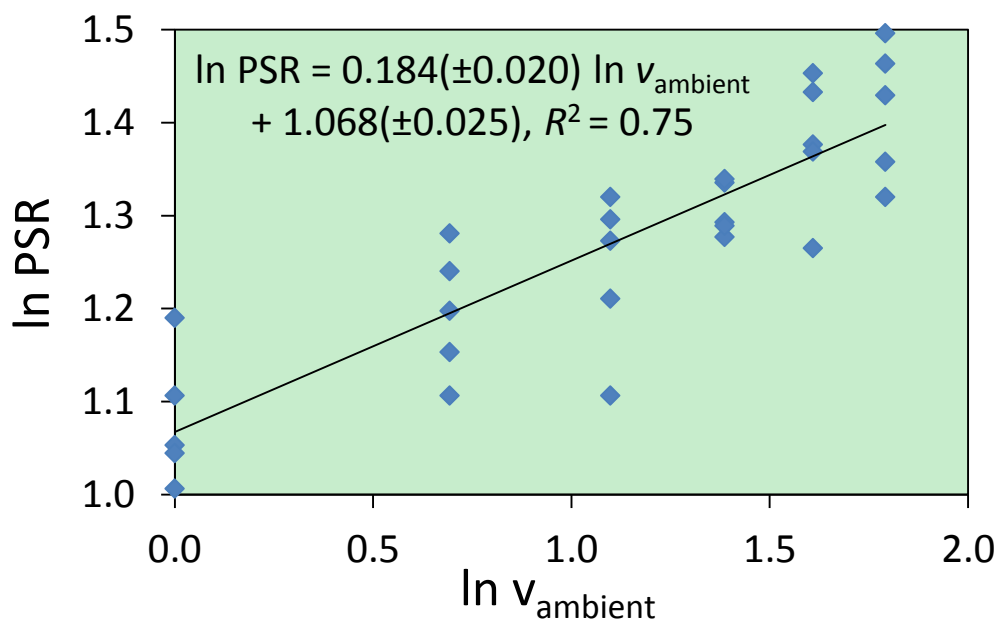
Figure S7. Linear fit of the natural logarithm transformed passive sampling rate (PSR) with ambient wind speed ($v_{ambient}$) from the water uptake experiments at different ambient wind speed.

Table S6. P-values of Turkey post-hoc multiple comparisons (significant level α=0.05) on passive sampling rates (based on water uptake by silica-gel) under wind of different angles.

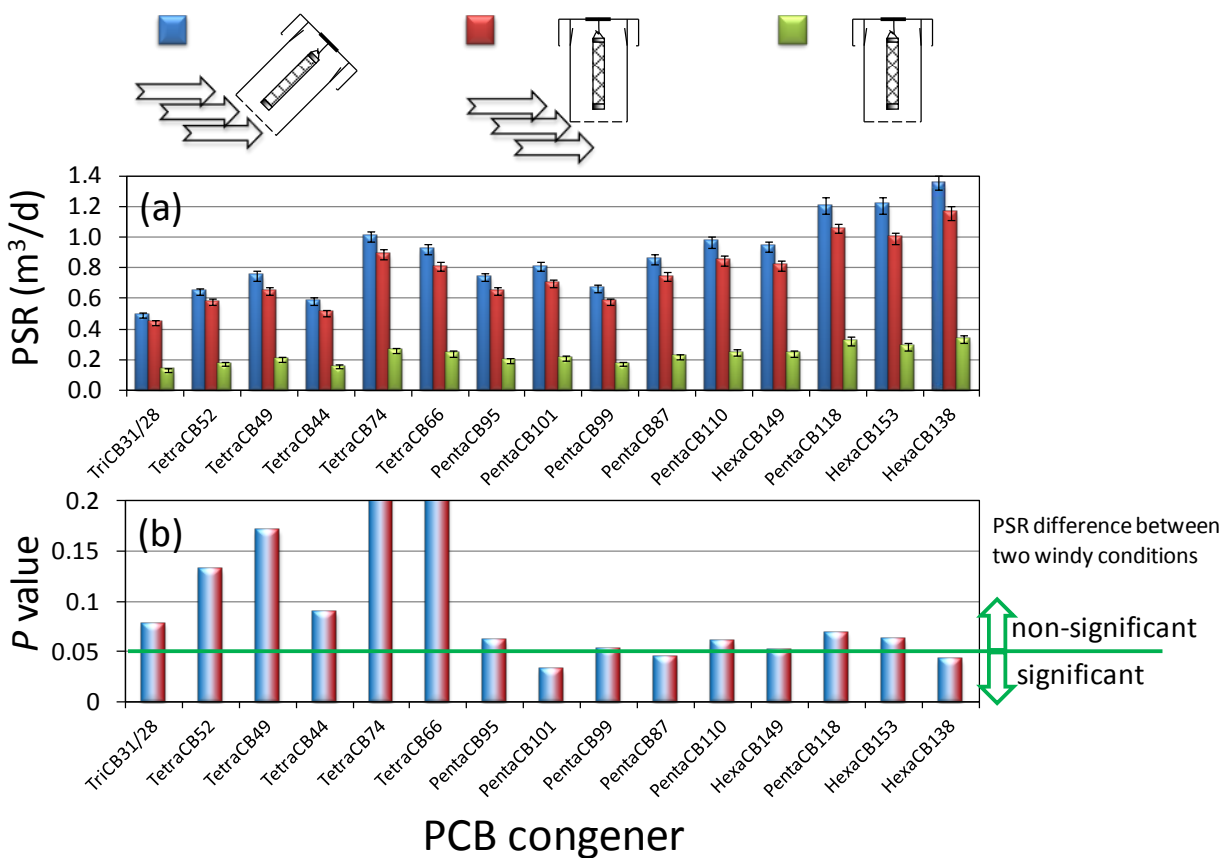| Wind angle (°)	0	15	30	45	-15	-30
0						
15	**0.050**					
30	0.060	1.000				
45	0.245	0.983	0.991			
-15	0.342	0.949	0.966	1.000		
-30	0.052	1.000	1.000	0.986	0.954	
-45	0.117	1.000	1.000	1.000	0.996	1.000

Figure S8. (a) Passive air sampling rates of PCBs under quasi wind still condition and with lab generated wind blowing at straight and 45° slanted angles towards the passive air samplers; (b) statistical test on the difference of passive air sampling rates between the two windy conditions
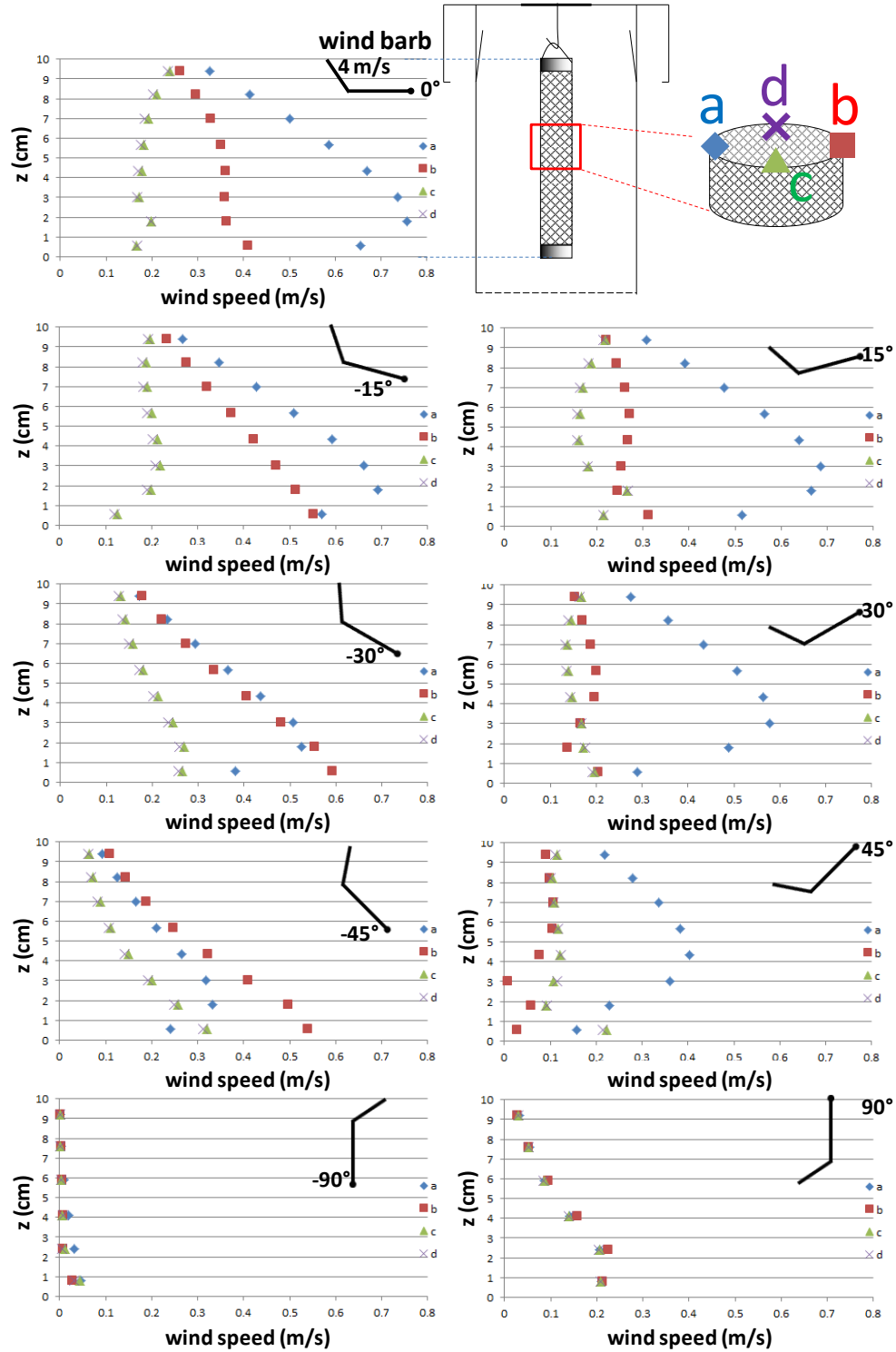
Figure S9. Computational fluid dynamic simulated air velocities around the passive sampling medium within the sampler housing with ambient winds blowing at different angles towards the passive sampler.
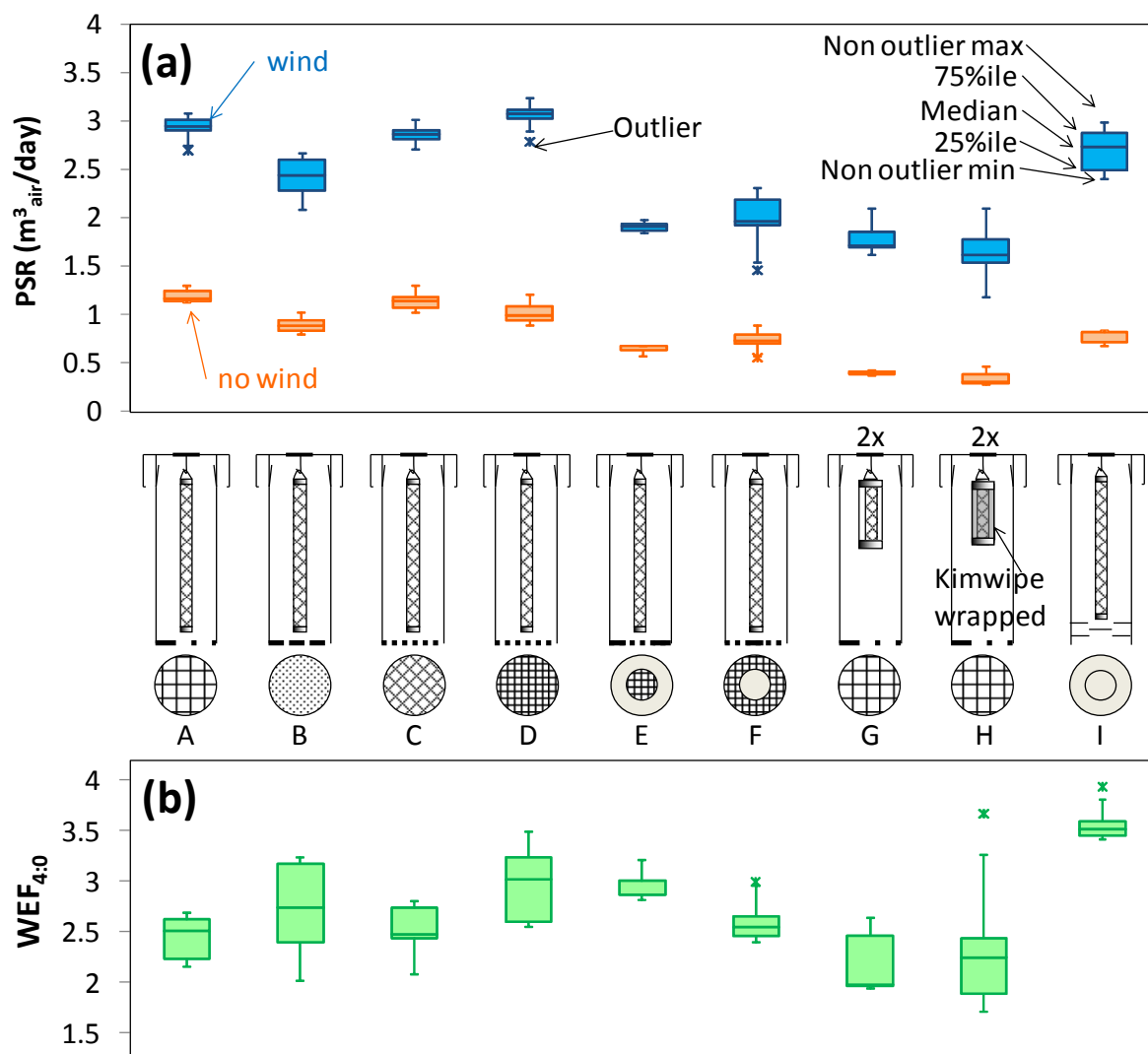
Figure S10. (a) Passive sampling rates based on water uptake by silica-gel under wind (4 m/s) and wind-still conditions for different sampler designs; (b) Influence of wind on passive sampling rates as indicated by the wind enhancement factor ($WEF_{4:0}$, the ratios between PSRs under the wind speed of 4 m/s and wind-still condition) for different sampler designs. The amounts of sorbent used for design G and H were half of the rest, so the PSRs were multiplied by two to be comparable.